J. Membrane Biol. 131, 115–127 (1993)

The Journal of
Membrane Biology

Anomalously Slow Mobility of Fluorescent Lipid Probes in the Plasma Membrane of the Yeast *Saccharomyces cerevisiae*

Miriam L. Greenberg† and Daniel Axelrod‡

†Department of Biological Sciences, Wayne State University, Detroit, Michigan and ‡Biophysics Research Division and Department of Physics, University of Michigan, Ann Arbor, Michigan 48109

Summary. We measured the lateral mobility of two fluorescent lipid probes dioctadecylindocarbocyanine (diI) and tetramethyl rhodamine phosphatidylethanolamine (R-PE) in the plasma membranes of *Saccharomyces cerevisiae inol* and *opi3* spheroplasts. These are well-characterized strains with mutations in the inositol and phosphatidylcholine biosynthetic pathways. Membrane phospholipid composition was altered by growing these mutants in the presence or absence of inositol and choline. Lateral mobility was measured by fluorescence recovery after photobleaching (FRAP). Microscopic fluorescence polarization employing CCD digital imaging produced an ordered orientation distribution of the lipid probe diI, confirming that at least one of the probes was largely incorporated into the bilayer membrane. Our results demonstrated anomalously slow mobility of both lipid probes for both mutants, regardless of whether the lipid composition was near normal or dramatically altered in relative composition of phosphatidylinositol and phosphatidylcholine. Trypsinization of the spheroplasts to remove surface proteins resulted in markedly increased lateral mobility. However, even in trypsinized spheroplasts, mobility was still somewhat lower than the mobility observed in the membrane of mammalian cells, such as rat smooth muscle culture cells tested here for comparison.

Key Words lipid diffusion · fluorescence recovery after photobleaching · carbocyanine · fluorescence polarization microscopy

Introduction

Lipids appear to have a high lateral mobility in most cell membranes, even in membranes in which protein motion is slow or restricted. As measured by fluorescence recovery after photobleaching (FRAP) (Axelrod et al., 1976), this high lipid mobility generally involves nearly 100% of the lipid probe and is characterized by a diffusion coefficient nearly two orders of magnitude greater than that of the mobile proteins in the same membrane (Jacobson, 1980, 1983; Vaz, Goodsaid-Salduondo & Jacobson, 1984; Edidin, 1987; Jacobson, Ishihara & Inman, 1987). Such observations tend to support the view of the membranes as a contiguous "sea of lipids" dotted only by mobile or immobile islands of protein. Lipid probe mobility in most cell membranes (reports ranging from about 2×10^{-9} to 2×10^{-8} cm^2/sec for a wide variety of natural cell systems) does seem to be slower than in artificial membrane systems (ranging from 2×10^{-8} to 6×10^{-8} cm^2/sec), but not nearly slow enough to suggest that the biological cell lipids are in a gel-like state or that the lipid probes are trapped in microdomains (Wolf et al., 1988). Rather, the slight retardation seems to increase with membrane protein concentration (Vaz et al., 1984). Significant changes in lipid composition (consistent with cell viability) seem to have only a marginal effect on the rapid lateral lipid probe diffusion in animal cells (Axelrod et al., 1978).

Nevertheless, in a few cases in vivo, lipids in membranes appear to be much less mobile than would be expected from a freely diffusive model (*see* Tocanne et al., 1989, for a review). In particular, unusually slow ($D < 1 \times 10^{-9}$ cm^2/sec) or only partial mobility (<70%) has been measured in the unusual double membranes of the parasite *Shistosoma mansoni* (Johnson et al., 1982; Foley et al., 1986) and nematodes *Trichinella spiralis* and *Toxicara canis* (Kennedy et al., 1987), as well as in rat L-cells (Zlatanov et al., 1987), and in distinct morphological regions of mammalian spermatozoa (Wolf et al., 1988). In some cases, the observation of lipid immobility is probe dependent, suggesting that different lipid probes may be reporting from different areas of the cell membrane and that perhaps some are not restricted exclusively to the membrane bilayer.

In this paper, we report an example in which the lipid mobility is anomalously low: in the plasma membrane of the yeast *Saccharomyces cerevisiae*. We measured lipid probe mobility in well-characterized mutant strains of this yeast which are blocked in the inositol and phosphatidylcholine biosynthetic

pathways. In these mutants, the relative composition of phosphatidylinositol and phosphatidylcholine can be manipulated by varying the concentration of exogenous inositol and choline. By examining the effect of lipid compositional changes, if any, on mobility, we hoped to narrow the range of possible causes of low lipid mobility.

We use *S. cerevisiae* yeast strains *ino1* and *opi3*. These mutants have been extensively characterized with respect to growth rate and phospholipid composition. The *ino1* mutant is defective in the conversion of glucose 6-phosphate to inositol 1-phosphate (Donahue & Henry, 1981). When supplied with exogenous inositol, the strain appears to grow as the wild type parent, exhibiting the same doubling time and membrane phospholipid composition. However, when starved for inositol, the relative composition of phosphatidylinositol (PI) in the cell membrane decreases dramatically (Henry et al., 1981). The *opi3* mutant is defective in the synthesis of phosphatidylcholine (PC) via methylation of phosphatidylethanolamine (Greenberg et al., 1983). When supplied with exogenous choline, membrane PC composition is half that of the wild type parent strain, and PI is twice that of the parent strain. When starved for choline, PC drops to 2% (*vs.* about 50% for the wild type), while the relative composition of mono- and di-methyl ethanolamine rises sharply (Greenberg et al., 1983). Thus, membranes of these two strains grown in the presence and absence of exogenous inositol and choline vary considerably with respect to relative phospholipid composition.

Our FRAP results show that lipid probe mobility in yeast membranes is anomalously low regardless of mutant type, for both of two different fluorophore probes. The observed immobility does not appear to arise from the yeast cell wall, since the measurements were performed on spheroplasts (yeast cells with the cell wall enzymatically digested). On the other hand, proteins do play a role in the immobilization since treatment with a proteolytic enzyme dramatically releases the restriction on lipid immobility.

We also demonstrate by a microscopic fluorescence polarization technique employing CCD digital imaging that at least one of the lipid probes we used is indeed largely incorporated into the yeast cell's bilayer membrane, producing a rather ordered orientation distribution. These polarization experiments argue against the possibility that the probe is predominantly internalized or adsorbed onto cell surface macromolecules or adhered as vesicles, all of which would likely produce a more random or uniform orientation distribution, and perhaps report an incorrect (and presumably much slower) mobility than exists in the bilayer. The polarization test used here is different and in some respects more stringent than previously used tests of membrane labeling based on accessibility to fluorescence quenching from the external solvent (Foley et al., 1986).

Materials and Methods

S. Cerevisiae Strains

The strains used in this study were the inositol auxotroph *ino1* (*ino1-13, ade1, MATα*), and phosphatidylcholine mutant *opi3* (*opi3-3, ade5, MATα*). Both strains have been extensively characterized previously with respect to membrane phospholipid composition (Henry et al., 1981; Greenberg et al., 1983).

Growth Media

Strains were maintained in 15% glycerol at −80°C for long-term storage and on YEPD (1% yeast extract, 2% peptone, 2% glucose) plates for short-term storage. For FRAP experiments, cells were grown in synthetic medium consisting of salts, vitamins, adenine, and glucose as previously described (Gaynor et al., 1991). Inositol (I) and choline (C) were added where indicated to 75 μM and 1 mM, respectively. I−, C− and I+, C+ denote the absence or presence of the respective chemical.

Growth of Cells

Synthetic medium containing inositol and choline was inoculated from a culture on a YEPD plate and incubated overnight at 30°C with aeration. Cells were washed twice in synthetic I− C− medium, resuspended in synthetic medium plus or minus I or C, and grown for five to seven generations.

Preparation of Spheroplasts

Cells were harvested by low speed centrifugation, washed once with spheroplast buffer (250 mM Tris-SO_4 pH 7.5, 1.2 M glycerol), resuspended to 10^6 to 10^7 cells/ml in 2 ml of spheroplast buffer containing 100 mM sodium thioglycolate and 4.02 mg zymolyase (20,000 U/g, ICN Immunobiologicals), and incubated at room temperature until spheroplasts were apparent (as monitored by lysis in dilute SDS). Spheroplasts were harvested, resuspended in buffer, and fluorescence labeled as described below.

Labeling with Fluorescent Probe

Two types of fluorescent lipid probes were used: 3,3′ dioctadecylindocarbocyanine (diI-C_{18}-(3), abbreviated diI; Molecular Probes); and N-(lissamine rhodamine B sulfonyl)dioleoyl phosphatidylethanolamine (R-PE; Avanti). Both types have the fluorophore group at the polar head of the molecules, and both are quite water insoluble. Each was dissolved at a concentration of about 0.5 mg/ml in 95% ethanol.

To 0.5 ml of the yeast cell suspension was added a quantity of the fluorescent lipid probe solution to produce a final concentration of either 2% or 6% ethanol (for R-PE) or 2% or 3% ethanol (for diI). (No significant differences in results were obtained for

these different concentrations of fluorescent label, so the results are combined for each fluorophore type.) Cells were then incubated for 5 min at 22°C and centrifuged at low speed. Excess solution was removed, 0.5 ml of fresh buffer was added, and the cells were vigorously agitated to resuspend them in the spheroplast buffer.

A droplet of the suspension was then placed on a fresh glass coverslip which just previously had been exposed to polylysine solution (Sigma) for 30 min at 22°C. The polylysine serves to coat the glass with positive charges onto which many of the cells settle and adhere strongly enough to suppress the obvious Brownian motion otherwise apparent on noncoated glass. The coverslip, with its aqueous bead of cell suspension, is mounted in an appropriate holder and placed on the stage of an inverted microscope for the FRAP experiments.

Most spheroplasts were slighly irregular spheres with labeling that qualitatively appeared to be localized on the surface, but with some unevenness of intensity and surface "hot spots" of sub-micron size.

Trypsinization

Some cells were treated with trypsin in order to maximally remove accessible surface proteins without destroying the cell's morphological integrity. We tested 0.25% trypsin [made by dilution of 2.5% trypsin (GIBCO) in spheroplast buffer] on *ino1* cells at 37°C. In one hour, the cell count as assayed in a hemocytometer dropped by 40% and in two hours by 95%. Therefore, prior to some FRAP experiments, we treated cells for one hour in trypsin at 37°C, with controls treated identically but in trypsin-free buffer. After subsequent labeling with 2% dil for 7 min at 22°C and mounting for observation, many of the trypsinized cells became flattened on the polylysine-coated surface and continued so well after removal of the trypsin; evidently their membranes had become very fragile. The trypsinized cells chosen for FRAP experiments were not checked for viability but were among those retaining their spherical shape although they were generally somewhat smaller than untrypsinized cells. These cells had few hot spots unlike untrypsinized spheroplasts, but the dil polarization effect indicating membrane incorporation (*see below*) was very obvious.

Comparison with Animal Cells

In order to compare the results for dil lipid diffusion with another eukaryotic cell, we labeled a culture dish of living rat smooth muscle cells, strain WKY (courtesy of Dr. David Bohr). The WKY cells were labeled in 2% dil/ethanol in phosphate buffered saline for 5 min at room temperature, washed, and observed by FRAP with the same optical system and objective as used for the yeast cells.

Fluorescence Recovery after Photobleaching

The FRAP experiments were performed in standard Gaussian spot photobleaching mode (Axelrod et al., 1976) through a 100× 1.25 NA Leitz oil immersion achromat objective on a Leitz Diavert microscope. A CW argon laser output at 514 nm, attenuated with neutral density filters, provided probe power estimated at approximately 10 μW at the sample. The bleach : probe intensity ratio, modulated by an acousto-optic modulator, was about 6000 : 1. The photomultiplier (Hamamatsu model R943-02) was operated with photon counting electronics (Pacific Instruments).

To convert FRAP recovery rates to calibrated diffusion coefficients, we assumed a e^{-2} focused spot radius w of 0.46 ± 0.04 μm, which was measured for the same objective in a similar optical system previously (Thompson & Axelrod, 1980).

Data acquisition and AOM control was handled by a 286-based 8 MHz MS-DOS PC equipped with a Metrabyte counter/timer board (CTM-05) and running custom Fortran and assembly language software. The sample bin for data acquisition was always set equal to the bleaching duration. Usually, this time was 2 msec; occasionally, times of 10 msec or 20 msec were used, with the incident beam correspondingly attenuated to maintain an approximately constant bleaching depth in all experiments of about 50% of the prebleach intensity. One complete scan consisted of 200 prebleach sample bins and 800 postbleach sample bins.

An adjustable square image plane diaphragm before the photomultiplier was closed down to an area just barely larger than the image of the fluorescent spot, so that the effective depth of light gathering was only about ±2 μm, significantly less than the thickness of a single yeast cell. It was thereby possible to gather FRAP data from either the upper or the lower surface of the cell. Since no significant differences were noted between the upper and lower surface results, they are combined in this report. The absence of a difference also argues that proximity to the polylysine substrate coating had no effect on probe mobility.

Because the recovery was far from complete for most samples, only one bleach/scan sequence was performed on each cell. To improve the statistical accuracy, the recovery curves gathered from cells under identical conditions (sample/bleach duration, probe type, and cell type) were then averaged together and are reported as a single set.

Fluorescence Polarization and dil Orientation

To estimate the fraction of dil that is incorporated in the bilayer rather than internalized or adsorbed to the exterior, we make use of the highly polarized excitation and emission as observed from dil incorporated in lipid bilayers (Yguerabide & Stryer, 1971; Badley, Martin & Schneider, 1973) and in cell membranes (Axelrod, 1979). A sample of *ino1* cells was labeled as above with 2% dil and allowed to settle on a glass coverslip as above. The cells were observed with an upright microscope through a 100× water immersion, 1.20 NA objective (Leitz) immersed directly into the bead of the aqueous buffer solution over the cells. The microscope emission path was equipped with two possible polarization filters, one oriented parallel and the other perpendicular to the excitation beam polarization direction. The polarized epi-illumination excitation light itself was the 514 nm line of a CW argon laser defocused to cover a large portion of the field of view. The detection system was a cooled CCD camera (Photometrics Star 1 system). From each of the two images (parallel $\parallel$ and perpendicular $\perp$ emission polarization) on each of seven cells (*see* an actual photograph with overlain schematic in Fig. 1), we recorded the intensities $F'_{N,E,S,W}(\parallel, \perp)$ at four positions on the circumference while focused at the plane of the equator: "north," "east," "south," and "west," where the north/south axis is the direction of the excitation polarization. An average intensity reading in each polarization from several nearby places on the background of each cell was subtracted to give a corrected fluorescence $F_{N,E,S,W}(\parallel,$

$\perp$). Finally, these fluorescence intensities are averaged pairwise together: $F_N(\|, \perp)$ and $F_S(\|, \perp)$ to form a fluorescence intensity $F_l(\|, \perp)$ along or "longitudinal" to the excitation polarization; $F_E(\|, \perp)$ and $F_W(\|, \perp)$ to form a fluorescence intensity $F_t(\|, \perp)$ across or "transverse" to the excitation polarization.

If each of the dil molecules was incorporated into the membrane bilayer and thereby oriented with its excitation and emission dipoles parallel to the spherical cell surface, then ideally the longitudinal intensities $F_l(\perp)$ and $F_l(\|)$ both would be zero because the excitation dipoles then would be orthogonal to the incident polarization. In addition, $F_t(\perp)$ would also be zero because the emission dipoles would be orthogonal to the emission polarization direction. Only $F_t(\|)$, with the orientation of both the excitation and emission dipoles in a favorable direction, would retain a nonzero intensity. If, on the other hand, some fraction of the dil was not incorporated in the bilayer, randomly oriented, and perhaps nonuniformly distributed around the cell surface, then $F_l(\perp)$ and $F_l(\|)$ and $F_t(\perp)$ would no longer be zero. As shown explicitly in the Appendix, one can calculate the fraction α of dil which is oriented (and thereby presumably in the bilayer) from the four measured intensities $F_{t,l}(\|, \perp)$. The Appendix also employs realistic corrections (based on Axelrod, 1979) for the high numerical aperture and the finite depth of light collection, both of which tend to decrease contrast between the bright $F_t(\|)$ and the dim $F_{t,l}(\perp)$ and $F_l(\perp)$.

FRAP Curve Fitting

The FRAP data (normalized in amplitude to its prebleach level) was fit to a theoretical function $f(t)$ appropriate to three diffusive components (immobile, slow, and fast), thereby involving five independent fitting parameters (the amplitudes $a_{1,2,3}$ of the immobile, slow, and fast components respectively, and the diffusion rates of the immobile, slow and fast components $r_{1,2,3}$, where the immobile rate r_1 is set equal to zero). The function assumes the incident beam is of Gaussian intensity cross-section and, as a simplifying approximation, that the bleaching depth is shallow. (The more general case of arbitrary bleaching depth, involving incomplete gamma functions, is also tractable but requires considerably more computational time for fitting.) The function can be written:

$$f(t) = 1 - \sum_{i=1}^{3} \frac{a_i}{1 + r_i t} \tag{1}$$

The fraction α_i of each component is given by:

$$\alpha_i \equiv a_i \Big/ \sum_{i=1}^{3} a_i \tag{2}$$

The fitting procedure was performed on a 486-based MS-DOS computer with a custom program based on the subroutines of Bevington (1969). When tested on simulated data, the program correctly returns input values as expected. The analysis of FRAP curves as a sum of three independent and discrete components fit all of the data very well as judged by eye. As judged mathematically, the reduced chi-squared was usually less than 1.1, with values of 1.27 and 9.3 in two cases. Since each set of the fitted data is an average over several cells, with the inherent biological variability in their probe mobility rates thereby obscured, a good mathematical fit to Eq. (1) should not necessarily be expected. Furthermore, a good mathematical fit, when it does occur, does not prove that exactly three physically discrete components (immobile, slow, and fast) exist. The physical truth may be a continuous range of rates with some characteristic distribution for which three distinct rates merely provide a good fit. Furthermore, the fitting procedure provides no restriction on the range of "slow" and "fast" components; e.g., a rate that is fit as "fast" on one curve may be similar to a rate fit as "slow" on another, but the fractions α may be such that these two curves are in fact quite similar. Likewise, the distinction between an "immobile" component and a very "slow" component can be sensitive to the duration of post bleach time used for fitting, because some of the longer characteristic recovery times approach the postbleach duration.

Because of these considerations, we report the results in two forms which summarize the fitted parameters in a manner which avoids arbitrary classifications and preserves the essence of the effects.

The first form is simply a three-point plot of α_i *vs.* r_i. When such a plot is skewed to the left, the sample consists largely of slow or immobile probes; when skewed to the right, the bulk of the probe is clearly more mobile. Differences in the distrubtion of mobilities among samples are very obvious in such a plot. The second form is cruder but even simpler: an average mobility $\langle r \rangle$:

$$\langle r \rangle \equiv \sum_{i=1}^{3} \alpha_i r_i \tag{3}$$

All of the rates r_i and $\langle r \rangle$ are reported as diffusion coefficients D, derived from the relationship

$$D = (\gamma/4) w^2 r \tag{4}$$

where γ is related to the bleaching depth and is approximately 1.2 here (Axelrod et al., 1976).

Results

Table 1 shows the fitted parameters for immobile, slow, and fast fractions $\alpha_{1,2,3}$, and the corresponding diffusion coefficients for the slow and fast fractions $D_{2,3}$ for each set of results gathered under identical conditions (same cell type, fluorophore, and sample/bleach time). The uncertainties (standard deviations from the mean) are calculated as part of the curve-fitting procedure and derive from photon statistical noise ("shot noise"). Note that results for sets with the same cell type and fluorophore type, but different sample/bleach time, sometimes differ by more than the photon uncertainty range. This is largely a real biological variability (from spot-to-spot), apparent when averaged curves from different sets of cells are separately curve-fit. The biological variability effect is not noticed within each set only because the individual FRAP curves comprising a set were summed together before curve-fitting to improve photon statistical accuracy.

The last column of Table 1 compares the single average parameter $\langle D \rangle$ (as calculated according to Eqs. (3) and (4) for each set. Although this kind of

Table 1. Three-component fits to FRAP data

Type probe sample time (msec)	n	Immobile	Slow		Fast		$\langle D \rangle$ (10^{-9} cm)
		α_1	α_2	D_2 (10^{-9} cm^2/sec)	α_3 (10^{-9} cm^2/sec)	D_3	
I+ dil 1	5	0.74 ± 0.03	0.13 ± 0.02	2.0 ± 0.8	0.13 ± 0.02	2.0 ± 0.8	0.52
I+ dil 2	4	0.45 ± 0.03	0.30 ± 0.07	1.6 ± 0.5	0.25 ± 0.07	1.6 ± 0.5	0.88
I+ dil 10	10	0.42 ± 0.01	0.35 ± 0.01	0.19 ± 0.02	0.23 ± 0.01	6.1 ± 1.1	1.5
I+ R-PE 2	6	0.66 ± 0.32	0.11 ± 0.11	0.03 ± 0.03	0.23 ± 0.02	14 ± 6	3.2
I− dil 2	4	0.86 ± 0.05	0.07 ± 0.07	0.4 ± 0.4	0.07 ± 0.07	0.4 ± 0.4	0.03
I− dil 10	4	0.44 ± 0.19	0.36 ± 0.19	0.02 ± 0.01	0.19 ± 0.01	4.2 ± 0.8	0.80
I− R-PE 2	6	0.42 ± 0.35	0.40 ± 0.35	0.11 ± 0.11	0.17 ± 0.02	20 ± 7	3.4
C+ R-PE 2	3	0.00 ± 0.01	0.78 ± 0.01	0.036 ± 0.003	0.22 ± 0.02	10 ± 5	2.2
C− R-PE 2	6	0.62 ± 0.04	0.22 ± 0.02	0.43 ± 0.20	0.15 ± 0.02	28 ± 16	4.3
TRYPdil 1	5	0.04 ± 0.01	0.60 ± 0.04	7.0 ± 0.9	0.36 ± 0.05	300 ± 300	108
RATdil 1	6	0.00 ± 0.00	0.03 ± 0.00	0.35 ± 0.04	0.97 ± 0.00	39.5 ± 0.2	38

Each entry line represents one FRAP curve consisting of a sum over n individual single-bleach FRAP curves taken on separate cells. The designations I+ and I− describe *inol* cells grown in the presence or absence of inositol and thus containing normal membranes or membranes with reduced phosphatidylinositol, respectively. The designations C+ and C− describe *opi3* cells grown in the presence or absence of choline, thus containing membranes with reduced phosphatidylcholine. TRYP are trypsin treated as described; RAT are rat smooth muscle cells in culture.

The uncertainties are standard deviations from the mean as produced by the Bevington (1969) curve-fitting procedure; they are generated from the photon statistical shot noise of the data points. However, the uncertainties of the various parameters can be correlated. A large uncertainty in α_1, for example, may be associated with a large uncertainty in α_2 if the fitting program cannot resolve well between immobility and very slow mobility with a very small D_2. For such runs, fitting functions with the diminished flexibility of only a single mobile component would return much smaller uncertainties but with slightly higher reduced χ^2 values. Uncertainties not apparent in each individual entry are due to (a) focused laser spot size which would only affect the means by the same multiplicative factor throughout; and (b) cell-to-cell variation. In some cases, fitting procedure located the best fit with "fast" and "slow" rates that are essentially equal, corresponding to only one mobile component.

In the Tryp dil case, there is evidence of a very fast initial component in the first three or four postbleach sample points. Due to the high shot noise inherent in so few and short sample times, the Bevington uncertainty procedure returns a very large uncertainty for D_3. The actual uncertainty is somewhat less; the Bevington procedure is mathematically not strictly applicable to large and asymetrically-distributed noise. Nevertheless, this curve can also be fit quite well (reduced $\kappa^2 = 1.04$) with a single mobile component function which simply smooths over the rapid initial postbleach rise; in that fit, $\alpha_1 = 0.07 \pm 0.01$; $\alpha_2 = 0.93 \pm 0.01$; and $D_2 = 10 \pm 1$. The consequent $\langle D \rangle = 9 \pm 1$ can be considered a lower limit because of the initial smoothing.

average into a single parameter is overly sweeping for a multicomponent system, and despite the obvious biological variability, the conclusion that lipid probes have a markedly restricted mobility in yeast cells is clear.

Because of the multiplicity of diffusion rates and fractions for each set, the results are also graphically presented in a form which makes their significance more readily apparent. The diffusion coefficients D_i and their corresponding fractions α_i are first averaged over all sets with identical cell and fluorophore type but different sample/bleach times (with a weighting according to the number of cells in each set). Figure 1 shows three-point plots of the resulting α_i *vs.* D_i (for $i = 1$ to 3) for each type of cell/fluorophore combination, with lines connecting the three points of each for clarity only. For cells with much immobility, we expect large α's to correspond to zero or low D_i's, thereby skewing the weight of the graph to the left. Conversely, cells with high mobility will have large α's corresponding to high D_i's, thereby skewing the graph to the right. It is clear that all of the yeast cell samples, whether I+, I−, C+, C−, or labeled with R-PE or with dil, have graphs skewed toward the immobile left. This skewing is especially clear when contrasted with: (*a*) the trypsinized I+ sample, which shows a significant shift to the mobile right and a very much diminished immobile fraction α_1; and (*b*) a rat (WKY strain) smooth muscle cell which shows dil to be highly mobile, much more typical of previous FRAP lipid mobility measurements on many types of cells (as reviewed in the Discussion).

Figure 2 shows actual summed FRAP curves for the trypsinized I+ cells and the directly comparable untrypsinized controls. The release of dil from an immobilized state by the protease treatment is quite clear.

Figure 3 shows a typical dil-labeled yeast spheroplast under polarized illumination and viewed with an emission polarizer (*a*) parallel and (*b*) perpendicular to the incident polarization. In the paral-

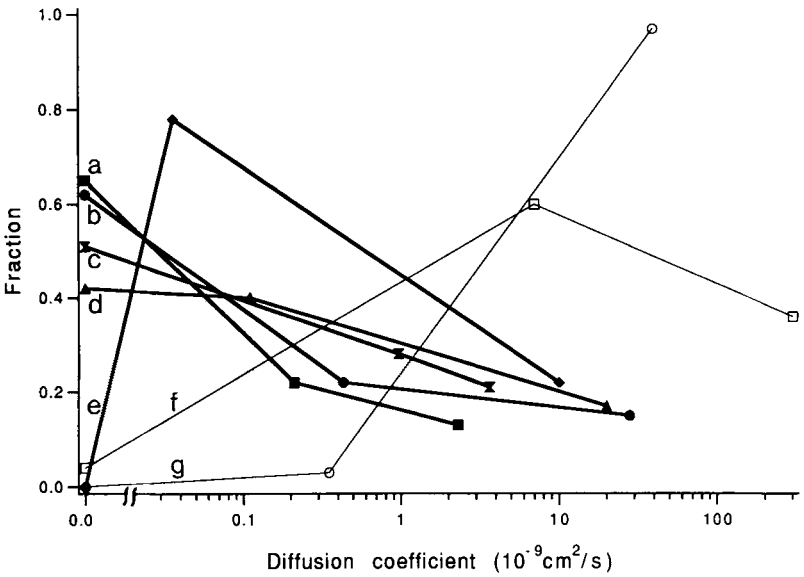

Fig. 1. Three-point plots of fitting parameters α_i *vs.* D_i, with connecting lines drawn as visual aids. For yeast mutants (heavy connecting lines), the graphs are identified with cell/fluorophore combinations as follows: (*a*) I−/dil; (*b*) C−/R-PE; (*c*) I+/dil; (*d*)I−/R-PE; (*e*) C+/R-PE. Two additional graphs of more mobile samples are included for comparison (light connecting lines): (*f*) trypsinized I+/dil; (*g*) rat smooth muscle/dil. The data are taken from the mean values shown in Table 1, with the I+/dil and I−/dil fitted parameters each averaged over their several sets with different sample times. The D_i axis is plotted on a pseudo-logarithmic scale to visually compress the high mobility end while retaining the spread among the slow mobilities. A break in the plot near the origin is provided to allow α_1 values of the immobile fraction ($D_1 = 0$) to appear on the ordinate axis.

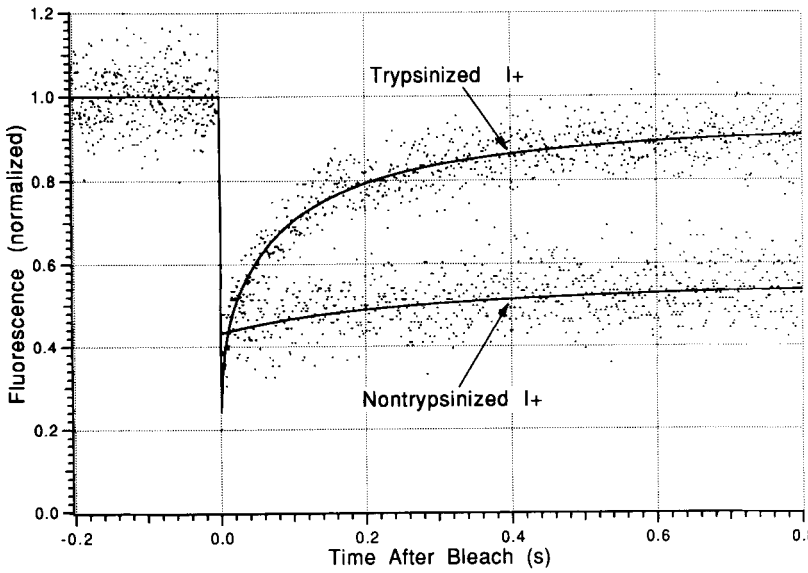

Fig. 2. Actual FRAP curves comparing trypsinized with nontrypsinized I+ cells labeled with dil. Each curve is a sum of FRAP experiments on five separate cells, with the prebleach fluorescence normalized to unity. This sum preserves the uncertainties due to photon shot noise but hides the uncertainties due to spot-to-spot (or cell-to-cell) variation. The solid lines are the curves generated by the fitting procedure.

lel view, the relative brightness around the "east" and "west" ends of the equator, and the relative darkness at the "north" and "south" poles is a qualitative indicator of some degree of orientation of the dil absorption and emission dipoles in a direction parallel to the cell surface. The Appendix, based on the theory presented in Axelrod (1979), outlines how intensity measurements at these four tangential points can be converted to a quantitative indication of the minimum fraction of dil (denoted as β) which is incorporated into the bilayer. From our measurements, we find that $\beta = 0.50 \pm 0.19$ (SD, $n = 7$).

Because oriented R-PE does not display a high emission polarization like dil, we cannot directly calculate an analogous minimum fraction of R-PE that is oriented in the plasma membrane.

If we assume that the fraction $(1 - \beta)$ of dil that is *not* oriented (and thereby may not be in the plasma membrane) is entirely immobile (say as adhered vesicles or as labeled and highly folded internal membranes or organelles), then our estimate of the fraction of immobility in the plasma membrane proper obviously would have to decrease. But even if such a correction was made to the immobile fractions shown in Fig. 1 (and thereby also increasing the mobile fractions), the lipid probe dil in yeast cells is

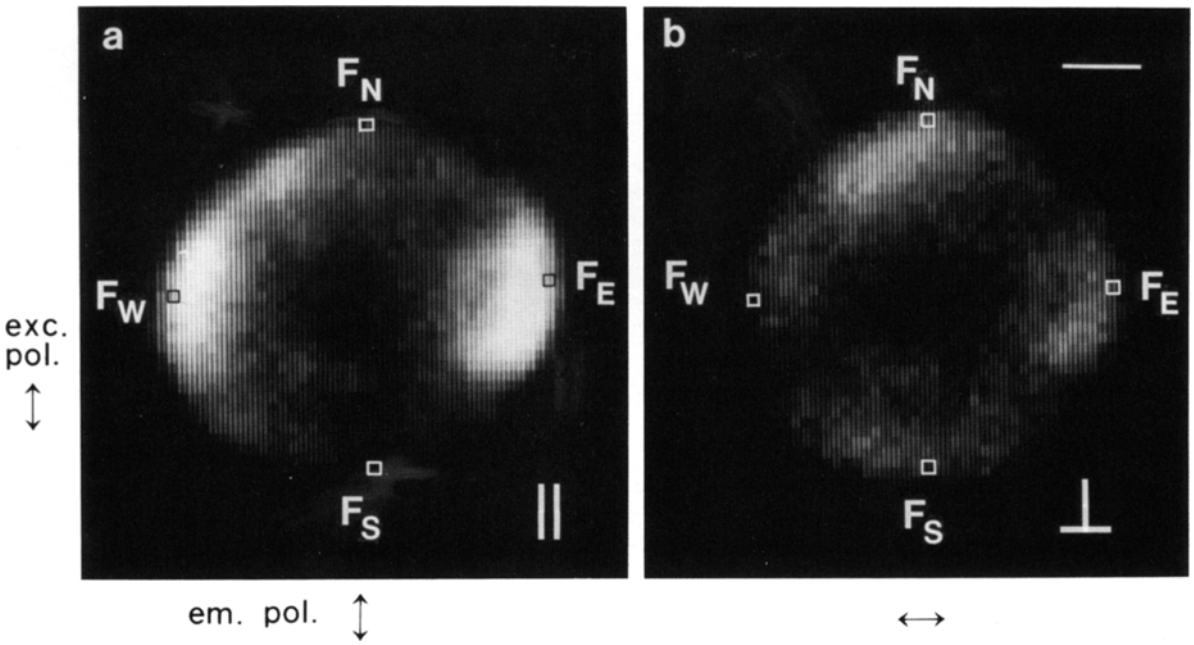

Fig. 3. Photographs of the CCD/video image of the same spheroplast labeled with diI, excited by 514 nm argon laser light polarized in the N–S direction and viewed through an emission polarizer in the (*a*) ∥ orientation (i.e., N–S); and (*b*) ⊥ orientation (i.e., E–W). The approximate locations of the pixels from which quantitative intensities $F_{N,B}(\|, \perp)$ are read are indicated. Readings from the "south" and "west" are averaged with those from the "north" and "east," respectively, and the averages are identified as F_N and F_E in the Appendix. The entire CCD image contains 384 × 576 pixels. With a 100× objective, the diameter of one yeast cell extends over only 35 pixels. The contrast in this reproduction is enhanced. Space bar = 1 μm.

still markedly less mobile than in the trypsinized sample or in rat smooth muscle cells.

Discussion

Measurements of fluidity in cell membranes can potentially contribute greatly to our understanding of the correlation between membrane structure and function. This approach would be especially useful in the model eukaryote *S. cerevisiae*, since it is such a tractable eukaryote, amenable to genetic, biochemical, and molecular analysis. Several techniques have been used to attempt to measure membrane fluidity in yeast membranes, including fluorescence polarization and EPR. Parks and coworkers compared the physical state of mitochondrial membranes from wild type and sterol mutant strains using fluorescence polarization (McLean-Bowen & Parks, 1981; Bottema, Rodriguez & Parks, 1985). Mishra and Prasad (1989) performed steady-state fluorescence polarization studies on the membranes of the unsaturated fatty acid mutant KD115. Their results indicate that "membrane fluidity" (as defined by the restricted rotational diffusion rate of a probe) is affected by the type of fatty acid supplement supplied to the cells and is correlated with amino acid transport rates. Several studies describe the use of electron paramagnetic spin labels to characterize ionic interactions between yeast membrane proteins and lipids (Henry & Keith, 1971; Henry, Keith & Snipes, 1976; Lees et al., 1979). However, neither the fluorescence polarization nor the electron spin resonance techniques measure lateral diffusion of lipids in membranes, and neither gave results that would suggest an anomalously low lateral mobility as measured here by FRAP.

Averaged over all the mutants, the mobility of the fluorescent lipid probes used here (R-PE and diI) is slower than that observed for similar probes on any other membrane system, and much slower than most (*see* Peters, 1981, for a review). The simplest one-parameter measure of diI lipid mobility is the average diffusion coefficient $\langle D \rangle$ (given by Eqs. (3) and (4) in units of 10^{-9} cm^2/sec). Our results for $\langle D \rangle$ on *S. cerevisiae* yeast along with most previously published FRAP results for carbocyanine and fluorescent-PE mobility on other intact cell membranes are summarized in Table 2.

Other anomalously low values for lipid mobility have been reported in the literature, but generally on cell surfaces that are not standard phospholipid

Table 2. Lipid probe mobility in cell surfaces

Cell	$\langle D \rangle$ (10^{-9} cm^2/sec)	Reference	Note
	Carbocyanine		
S. cerevisiae yeast	0.7 ± 0.5 (SD)	This paper	[a]
Rat smooth muscle	38	This paper	
Human erythrocyte ghosts	1.5	Thompson & Axelrod, 1980	[b]
Human lymphocytes	4.5	Thompson & Axelrod, 1980	[b]
Rat fibroblasts	9	Thompson & Axelrod, 1980	[b]
Chick primary myotubes	4	Axelrod et al., 1978	
Rat L6 myoblasts	9	Schlessinger et al., 1977	
Mouse spleen lymphocytes	10–17	Dragsten et al., 1979	
Human lymphocytes	8	Dragsten et al., 1979	
Human erythrocytes	8	Bloom & Webb, 1983	
Mouse erythrocytes	13	Bloom & Webb, 1983	
Inner mitochondrial membrane	5	Reviewed in Vaz et al., 1984	
Fibroblasts	10	Reviewed in Vaz et al., 1984	
Sickled erythrocytes	7	Boullier et al., 1986	
Chicken embryo fibroblast	3	Elson & Yguerabide, 1979	
Mouse neuroblastoma	2–6	DeLaat et al., 1980	
3T3 mouse fibroblast	8	Eldridge, Elson & Webb, 1980	
3T3 mouse fibroblast	5	Wolf, Henkart & Webb, 1980	
Unfertilized sea urchin eggs	6	Peters, Sardet & Richter, 1984	
Fertilized sea urchin eggs	2.2	Peters & Richter, 1981	
Mouse spermatazoa	0.7	Wolf, 1987	[c]
Ram spermatazoa	2.2	Wolf et al., 1988	[c]
Rats testes L-cells	0.2	Zlatanov et al., 1987	[d]
	Fluorescent-PE		
S. cerevisiae yeast	3.3 ± 0.9 (SD)	This paper	[e]
Human PMN leukocytes	23	Petty et al., 1980	
Ram spermatazoa	3.5	Wolf et al., 1988	[c]
Intact erythrocytes	4.5	Golan et al., 1988	
Mouse erythrocyte ghosts	15	Koppel, Sheetz & Schindler, 1981	

[a] Averaged over all five sets using dil listed in Table 1.
[b] Obtained on our equipment using similar optics to that for the present yeast experiments. Exact comparison of results between different labs must be viewed somewhat cautiously because of spot size uncertainties.
[c] Spermatazoa show a lipid mobility which is dependent on both the physiological stage and the region of this highly segmented cell. These are the minimum values reported.
[d] In this case, other lipid probes and even protein probes were seen to move about ten times *faster* than dil, so it is possible that dil was not reporting from all significant portions of the bilayer.
[e] Averaged over all four sets using R-PE listed in Table 1.

single bilayers. On the corrugated outer membrane of the body section of the parasitic worm *Schistosoma mansoni*, $\langle D \rangle$ is reported as low as 0.6 for carbocyanine and 0.1 for fluorescein-PE, and on the immature *Schistosomula*, as low as 0.1 for carbocyanine (Foley et al., 1986). However, in these cases, the distribution of dil in the complex three bilayer skin of this worm is not certain, the membrane is far from planar, and the probe produces a highly patterned fluorescent staining on the worm's body. Probably the lowest reported lipid lateral mobility in any cell surface system with any probe is for a fluorescein-labeled fatty acid in the epicuticle of the parasitic nematodes *Trichinella spiralis* and *Toxicara canis*, with virtually complete immobility (Kennedy et al., 1987). However, the nematode epicuticle is structurally quite different from a cellular plasma membrane.

Our value for rhodamine-PE mobility on yeast is considerably higher than that for dil, but still slow relative to most probes on most cells. Both the carbocyanine and R-PE probes obviously see a yeast membrane in which lipid motion is quite restricted, but they may partition somewhat differently in different regions or microdomains.

The fitted parameter results show that the means

vary significantly from run-to-run on the same cell type; the variations exceed the random statistical uncertainty of photon shot noise although they are not nearly large enough to obscure the overall immobilization effect. These variations are probably real: different cells, and probably different locations on the same cell, have a real spread in lipid mobility. This effect appears to exist in lipid probe mobility experiments from other labs as well. The variation may be a reflection of a domain structure of micron size or larger. Only a very few FRAP studies specifically address possible microdomains (e.g., Yechiel & Edidin, 1987), but it is worth further study. There may well be some average difference in $\langle D \rangle$ between different yeast lipid mutants, but the difference is probably less than the variations on a single cell. Tens or hundreds of averaged experiments can always reduce the reported standard error far enough to reveal such small differences but they may not be functionally significant in view of the large and real biological variabilities.

Another uncertainty is in the reported uncertainties themselves. A small difference in the actual shape and rate of a recovery curve can lead to a large difference in the relative assignment of fractions and rates among, for example, the immobile and slow components. This sensitivity of multicomponent fitting to small shape changes leads to large reported uncertainties, but these uncertainties are statistically interdependent among components.

Despite the complexity of the multicomponent fitting scheme, it is still best to use a fitting function that ignores neither rapid nor immobile components. The plot of α_i *vs.* $\langle D_i \rangle$ shown in Fig. 1 is somewhat unique for reporting FRAP results, but it seems to graphically depict the essence of the results without burying the multicomponent nature or the cell-to-cell variability.

In any studies using lipid probes, there is always a question about the distribution of the probe, since neither the exact mechanism of incorporation of a hydrophobic probe from a vesicle into a biological cell nor the subsequent transport processes are well understood. Furthermore, even the qualitative appearance of surface labeling (brightness tangentially around the surface) does not rule out labeling of hydrophobic regions within a light-resolution distance from the membrane, such as sub-membrane proteins, endoplasmic reticulum, extracellular glycoproteins, or (in our case) any possible remains of cell wall left undigested by zymolyase. For this reason, it is important to have an independent and quantitative assay of true membrane incorporation. One method used in previous FRAP studies (Foley et al., 1976; Kennedy et al., 1987) tests for accessibility to membrane-impermeant fluorescence quenchers. This method has the virtue that, if quenching is complete, internal labeling of the cell can be completely ruled out. Unfortunately, for several probes such as diI and labeled-PE, quenching is not complete. The source of the remaining unquenched fluorescence then cannot be distinguished between the inner leaflet of the bilayer or more deeply internal structures. And in any case, the quenching method cannot distinguish between quench-accessible fluorophores in the outer leaflet of the bilayer and those adsorbed elsewhere on the outside. Adsorbed probe vesicles are said to not contribute because they self-quench, but the self-quenching is not complete.

For these reasons, we chose a somewhat more stringent test of membrane incorporation, based on the orientational distribution of the absorption and emission transition dipole moments in the head group of the probe. We assume that probe molecules incorporated into the bilayer would be highly oriented, with the hydrocarbon tails of the probe parallel to those of the phospholipids in the bilayer. In the case of diI, this would place the linear conjugated bridge of the indocarboxycyanine head group and its transition dipoles parallel to the cell surface. Conversely, no other distribution of diI with its dipoles parallel to the surface (e.g., the whole molecule including the hydrocarbon tails lying flat on the surface) seems thermodynamically stable. In the case of R-PE, the dipoles are not so fixed relative to the hydrocarbon tail direction, so R-PE is not amenable to this test.

Under polarized illumination and detection optics, the diI labeling pattern appears as a polar anisotropic intensity distribution around the periphery of a spherical cell, one that is quantitatively predictable from a theory that takes into account the finite objective aperture, rotational diffusion of the diI, the finite viewing depth at the edge of the cell, and nonparallelism of the absorption and emission dipoles (Axelrod, 1979). We then assume that any fraction of the diI that is not incorporated into the bilayer is randomly oriented on the light-microscopic distance scale, so that fraction displays a uniform, isotropic intensity around the cell periphery. By comparing the measured intensity anisotropy around the edge with a theory combining contributions from the oriented and disoriented fractions, we calculate the average fraction that is oriented and thereby presumably incorporated in the bilayer (either leaflet).

We find that approximately 50% of the diI is oriented. The most conservative interpretation of our results would be to assume that a full 50% of the diI was not in the membrane bilayer and that this 50% was totally immobile. Then the average $\langle D \rangle$ values for those diI molecules in the bilayer would be doubled at most. This would still give a value

much less than $\langle D \rangle$ for most other cell types. Note that these other $\langle D \rangle$ values would also need to be corrected in a similar manner to account for a nonbilayer immobile fraction, also resulting in an increased $\langle D \rangle$ for diI in the bilayers of those other cells. Unfortunately, most other cells are not sufficiently regular in shape (e.g., spherical) for the polarization method to yield a value for the nonbilayer fraction.

Several possibilities might account for the striking immobility we observed in yeast membranes compared to those of mammalian cells. One possibility is that immobility is due to some aspect of lipid composition that is unique to yeast membranes. However, significant alterations in the lipid composition of the plasma membranes of other living cells produces only moderate changes in the lateral mobility of lipid probes and does not immobilize them (Axelrod et al., 1978). Furthermore, yeast membranes are fairly typical of those of higher eukaryotes with respect to membrane phospholipid content (Henry, 1982). One difference between yeast and mammalian phospholipids, however, is that *S. cerevisiae* sphingolipids are inositol-containing, in contrast to the sphingolipids found in mammalian cells (Smith & Lester, 1974). The yeast sphingolipids are hydroxylated and contain C26 fatty acids, and are highly localized to the plasma membrane (Patton & Lester, 1991). Whether the unique sphingolipid composition might account for some of the relative immobility we observed is a hypothesis that is testable by FRAP analysis of the sphingolipid-defective yeast mutant described by Wells & Lester (1983). However, it is difficult to imagine how this alone could account for the increase in mobility that we observed following treatment of the spheroplasts with trypsin. In general, it has been noted that lipid probes diffuse considerably faster in protein-free artificial bilayer systems than in almost any cell membrane (Jacobson, 1980).

Another explanation for immobility is that yeast membrane protein composition is greater than that of mammalian cells. It is clear that increased protein concentration in artificial and natural membranes is correlated with sterically hindered diffusion of proteins and lipids (reviewed in Vaz et al., 1984). This might account for the increase in lipid diffusion we observed following trypsinization. However, there is no evidence that yeast membrane protein content is significantly greater than that of higher eukaryotes to an extent that could account for the steric hindrance effect to apply here. Interestingly, in one of the only reported examples of lipid immobility in mammalian cells (differentiating sperm cells), removing surface proteins with pronase does not affect lipid diffusion, nor is lipid diffusion increased in bilayers prepared from protein-free lipid extracts of sperm membranes (Wolf, Lipscomb & Maynard, 1988).

It is conceivable that the low lipid mobility is somehow due to interactions of the lipid, directly or indirectly, with the cell wall. This seems unlikely because of the prior disruption of the cell wall by zymolase. However, we cannot rule out the possibility that cell wall fragments remain which are further disrupted by our trypsin treatment.

The hypothesis that we believe most likely to account for lipid immobility in yeast membranes is that lipids, in addition to proteins, are not homogeneous in the membrane but rather exist in sub-micron size microdomains (for a review of this idea, *see* Lentz, 1988). One example of such a microdomain is a cage of proteins configured in arrays that trap the lipids within. If the size of the cage is smaller than the size of the focused laser beam, then the slow mobility we observed represents movement of lipids between cages. In the case of yeast, a microdomain must be somehow associated with protein in light of the release of immobility by trypsin. (Nonetheless, the association could be quite indirect, involving several steps of cellular alteration after proteolysis.) Therefore, a simple lipid phase separation, as observed in artificial pure lipid membrane systems, cannot account for the putative microdomains in yeast. The possibility that yeast lipids are trapped in cages that permit short-range motions but restrict long-range motions is testable; the rotational diffusion of lipids (which is sensitive to environment only on a molecular size scale) in yeast could be compared with that in other cells that have a higher translational lipid mobility.

The possibility of sub-micron sized lipid domains extends inferences drawn from mobility results on other systems. Sea urchin and mouse egg membranes appear to be composed of domains which are altered upon fertilization (Wolf, Edidin & Handyside 1981; Wolf et al., 1981). Microdomains of the sperm plasma membrane may account for restricted lipid diffusion on the morphologically distinct regions of the sperm surface (Wolf, 1987), although that restriction is not relieved by protease treatment in contrast to our observation in yeast. The measured value for lipid probe diffusion rate in fibroblasts has been found to be dependent on spot size and spot location, an effect which can be interpreted as arising from lipid domains of micron-size scale (Yechiel & Edidin, 1987). Micron-size compartmentalization of proteins, rather than lipids, is more well known. For example, in *E. coli*, compartmentalization of the periplasm is related to regions specialized for cell division (Foley et al., 1989). Acetylcholine receptors are localized in tens-of-micron-

sized clusters on developing rat myotubes (Bloch et al., 1989). Newly synthesized chemotaxis signal transducer MCP, an integral membrane receptor protein, is localized to the nascent swarmer cell portion of the predivisional cell in *Caulobacter crescentus* (Nathan et al., 1986).

In conclusion, we have shown that lateral diffusion of lipids in *S. cerevisiae* membranes is among the slowest observed in a higher eukaryotic membrane. Lipid diffusion increases upon removal of surface proteins with trypsin. Our data are consistent with the hypothesis that lipids have a spectrum of mobilities that range over orders of magnitude, depending upon their microdomain within the membrane. In addition, from an experimental viewpoint, the slow rate of lipid diffusion suggests that yeast may be a good system in which to study accretion of labeled lipids into organelles.

We thank Dr. Robert M. Fulbright for his invaluable help with curve-fitting and production of the line drawings, Dr. David Bohr for providing the WKY rat smooth muscle cells used for comparison, and Drs. Nancy L. Thompson, Geneva Omann, and Amiya Hajra for useful discussions. This work was supported by NIH NS14565 and NSF DMB8805296 (to D.A.) and NIH GM37723 (to M.G.).

References

Axelrod, D. 1979. Carbocyanine dye orientation in red cell membrane studied by microscopic fluorescence polarization. *Biophys. J.* **26**:557–573

Axelrod, D., Koppel, D.E., Schlessinger, J., Elson, E. Webb, W.W. 1976. Mobility measurements by analysis of fluorescence photobleaching recovery. *Biophys. J.* **16**:1055–1069.

Axelrod, D., Wight, A., Webb, W., Horwitz, A. 1978. Influence of membrane lipids on acetylcholine receptor and lipid probe diffusion in cultured myotube membrane. *Biochemistry* **17**:3604–3609.

Badley, R.A., Martin, W.G., Schneider, H. 1973. Dynamic behavior of fluorescent probes in lipid bilayer model membranes. *Biochemistry* **12**:268–275.

Bevington, P.R. 1969. Data Reduction and Error Analysis for the Physical Sciences. McGraw-Hill, New York

Bloch, R.J., Velez, M., Krikorian, J., Axelrod, D. 1989. Microfilaments and actin-associated proteins at sites of substrate attachment in acetylcholine receptor clusters of cultured rat myotubes. *Exp. Cell Res.* **182**:583–596

Bloom, J.A., Webb, W.W. 1983. Lipid diffusibility in the intact erythrocyte membrane. *Biophys. J.* **42**:295–305

Bottema, C.D.K., Rodriguez, R.J., Parks, L.W. 1985. Influence of sterol structure on yeast plasma membrane properties. *Biochim. Biophys. Acta* **813**:313–320

Boullier, J.A., Brown, B.A., Bush, J.C., Jr., Barisas, G.B. 1986. Lateral mobility of a lipid analog on the membrane of irreversible sickle erythrocytes. *Biochim. Biophys. Acta* **856**:301–309

De Laat, S.W., Van der Saag, P.T., Elson, E.L., Schlessinger, J. 1980. Lateral diffusion of membrane lipids and proteins during the cell cycle of neuroblastoma cells. *Proc. Natl. Acad. Sci. USA* **77**:1526–1528

Donahue, T.F., Henry, S.A. 1981. Myoinositol-1-phosphate synthase: Characteristics of the enzyme and identification of its structural gene in yeast. *J. Biol. Chem.* **256**:7077–7085

Dragsten, P., Henkart, P., Blumenthal, R., Weinstein, J., Schlessinger, J. 1979. Lateral diffusion of surface immunoglobulin, Thy-1 antigen, and a lipid probe in lymphocyte plasma membranes. *Proc. Natl. Acad. Sci. USA* **76**:5163–5167

Edidin, M. 1987. Rotational and lateral diffusion of membrane proteins and lipids: phenomena and function. *Curr. Top. Membr. Transp.* **29**:91–127

Eldridge, C.A., Elson, E.L., Webb, W.W. 1980. Fluorescence photobleaching recovery measurements of surface lateral mobilities on normal and SV40-transformed mouse fibroblasts. *Biochemistry* **19**:2075–2079

Elson, E.F., Yguerabide, J. 1979. Membrane dynamics of differentiating cultured embryonic chick skeletal muscle cells by fluorescence microscopy techniques. *J. Supramol. Struct.* **12**:47–61

Foley, M., Brass, J.M., Birmingham, J., Cook, W.R., Garland, P.B., Higgins, C.F., Rothfield, L.I. 1989. Compartmentalization of the periplasm at cell division sites in *Escherichia coli* as shown by fluorescence photobleaching experiments. *Mol. Microbiol.* **3**:1329–1336

Foley, M., Kusel, J.R., Garland, P.B. 1988. Changes in the organization of the surface membrane upon transformation of ceracariae to schistosomula of the helminth parasite *Schistosoma mansoni*. *Parasitology* **96**:85–97

Foley, M., MacGregor, A.N., Kusel, J.R., Garland, P.B., Downie, T., Moore, I. 1986. The lateral diffusion of lipid probes in the surface membrane of *Schistosoma mansoni*. *J. Cell. Biol.* **103**:807–818

Gaynor, P.M., Hubbell, S., Schmidt, A.J., Lina, R.A., Minskoff, S.A., Greenberg, M.L. 1991. Regulation of phosphatidylglycerolphosphate synthase in *Saccharomyces cerevisiae* by factors affecting mitochondrial development. *J. Bacteriol.* **173**:6124–6131

Golan, D.E., Furlong, S.T., Brown, C.S., Caulfield, J.P. 1988. Monopalmitoylphosphatidylcholine incorporation in human erythrocyte ghost membranes causes protein and lipid immobilization and cholesterol depletion. *Biochemistry* **27**:2661–2667

Greenberg, M.L., Klig, L.S., Letts, V.A., Shicker Loewy, B., Henry, S.A. 1983. Yeast mutant defective in phosphatidylcholine synthesis. *J. Bacteriol.* **153**:791–799

Henry, S.A. 1982. Membrane lipids of yeast: biochemical and genetic studies. *In*: The Molecular Biology of the Yeast Saccharomyces: Metabolism and Gene Expression. J.N. Strathern, E.W. Jones, J.R. Broach, editors. pp. 101–158. CSH Biol. Lab., Cold Spring Harbor

Henry, S.A., Greenberg, M.L., Letts, V., Shicker, B., Klig, L., Atkinson, K.D. 1981. Genetic regulation of phospholipid synthesis in yeast. *In:* Current Developments in Yeast research: Advances in Biotechnology. G. Stewart and J. Russell editors. pp. 311–316. Pergamon, New York

Henry, S.A., Keith, A.D. 1971. Membrane properties of saturated fatty acid mutants of yeast revealed by spin labels. *Chem. Phys. Lipids* **7**:245–265

Henry, S.A., Keith, A.D., Snipes, W. 1976. Changes in the restriction of molecular rotational diffusion of water-soluble spin labels during fatty acid starvation of yeast. *Biophys. J.* **16**:641–653.

Jacobson, K. 1980. Fluorescence recovery after photobleaching: lateral mobility of lipids and proteins in model membranes and on single cell surfaces. *In:* Lasers in Biology and Medicine,

ed. F. Hillenkamp, R. Pratesi, and C.A. Sacchi editors. pp. 271–288. Plenum, New York

Jacobson, K. 1983. Lateral diffusion in membranes. *Cell Motil.* **3:**367–373

Jacobson, K., Ishihara, A., Inman, R. 1987. Lateral diffusion of proteins in membranes. *Annu. Rev. Physiol.* **49:**163–175

Johnson, P., Garland, P.B., Campbell, P., Kusel, J.R. 1982. Changes in the properties of the surface membrane of *Schistosoma mansoni* during growth as measured by fluorescence recovery after photobleaching. *FEBS Lett.* **141:**132–135

Kennedy, M.W., Foley, M., Kuo, Y.-M., Kusel, J.R., Garland, P.B. 1987. Biophysical properties of the surface lipid of parasitic nematodes. *Mol. Biochem. Parasitol.* **22:**233–240

Lees, N.D., Bard, M., Kemple, M.D., Haak, R.A., Kleinhans, F.W. 1979. ESR determination of membrane order parameter in yeast sterol mutants. *Biochim. Biophys. Acta* **553:**469–475

Lentz, B.R. 1988. Organization of membrane lipids by intrinsic membrane proteins. *In:* Lipid Domains: the Relationship to Membrane Function. pp. 141–161. Alan R. Liss, New York

McLean-Bowen, C.A., Parks, L.W. 1981. Corresponding changes in kynurenine hydroxylase activity, membrane fluidity, and sterol composition in *Saccharomyces cerevisiae* mitochondria. *J. Bacteriol.* **143:**1325–1332

Koppel, D.E., Sheetz, M.P., Schindler, M. 1981. Matrix control of protein diffusion in biological membranes. *Proc. Natl. Acad. Sci. USA* **78:**3576–3580

Mishra, P., Prasad, R. 1989. Relationship between fluidity and L-alanine transport in a fatty acid auxotroph of *Saccharomyces cerevisiae*. *Biochem. Int.* **19:**1019–1030

Nathan, P., Gomes, S.L., Hahnenberger, K., Newton, A., Shapiro, L. 1986. Differential localization of membrane receptor chemotaxis proteins in the *Caulobacter* predivisional cell. *J. Mol. Biol.* **191:**433–440

Patton, J.L., Lester, R.L. 1991. The phosphoinositol sphingolipids of *Saccharomyces cerevisiae* are highly localized in the plasma membrane. *J. Bacteriol.* **173:**3101–3108

Peters, R. 1981. Translational diffusion in the plasma membrane of single cells as studied by fluorescence microphotolysis. *In:* Cell Biology International Reports. pp. 733–760. Academic, London

Peters, R., Richter, H.-P. 1981. Translational diffusion in the plasma membrane of sea urchin eggs. *Dev. Biol.* **86:**285–293

Peters, R., Sardet, C., Richter, H.-P. 1984. Mobility of membrane lipids and proteins at the animal and vegetal pole of the sea urchin egg. *Dev. Growth Differ.* **26:**105–110

Petty, H.R., Smith, L.M., Fearon, D.T., McConnell, H.M. 1980. Lateral distribution and diffusion of the C3b receptor of complement, HLA antigens, and lipid probes in peripheral blood leukocytes. *Proc. Natl. Acad. Sci. USA* **77:**6587–6591

Schlessinger, J., Axelrod, D., Koppel, D.E., Webb, W.W., Elson, E.L. 1977. Lateral transport of a lipid probe and labeled proteins on a cell membrane. *Science* **195:**307–309

Smith, S.W., Lester, R.L. 1974. Inositol phosphorylceramide, a novel substance and the chief member of a major group of yeast sphingolipids containing a single inositol phosphate. *J. Biol. Chem.* **249:**3395–3405

Thompson, N.L., Axelrod, D. 1980. Reduced lateral mobility of a fluorescent lipid probe in cholesterol-depleted erythrocyte membrane. *Biochim. Biophys. Acta* **597:**155–165

Tocanne, J.-F., Dupou-Czanne, L., Lopez, A., Tournier, J.-F. Lipid lateral diffusion and membrane organization. *FEBS Lett.* **257:**10–16

Vaz, W.L.C., Goodsaid-Zalduondo, F., Jacobson, K. 1984. Lateral diffusion of lipids and proteins in bilayer membranes. *FEBS Lett.* **174:**199–207

Wells, G.B., Lester, R.L. 1983. The isolation and characterization of a mutant strain of *Saccharomyces cerevisiae* that requires a long chain base for growth and for synthesis of phosphosphingolipids. *J. Biol. Chem.* **258:**10200–10203

Wolf, D.E. 1987. Diffusion and the control of membrane regionalization. *Ann. NY Acad. Sci.* **513:**247–261

Wolf, D.E., Edidin, M., Handyside, A.H. 1981. Changes in the organization of the mouse egg plasma membrane upon fertilization and first cleavage: Indications from the lateral diffusion rates of fluorescent lipid analogs. *Dev. Biol.* **85:**195–198

Wolf, D.E., Henkart, P., Webb, W.W. 1980. Diffusion, patching, and capping of stearoylated dextrans on 3T3 cell plasma membranes. *Biochemistry* **19:**3893–3904

Wolf, D.E., Kinsey, W., Lennarz, W., Edidin, M. 1981. Changes in the organization of the sea urchin egg plasma membrane upon fertilization: Indications from the lateral diffusion rates of lipid soluble fluorescent dyes. *Dev. Biol.* **81:**133–138

Wolf, D.E., Lipscomb, A.C., Maynard, V.M. 1988. Causes of nondiffusing lipid in the plasma membrane of mammalian spermatozoa. *Biochemistry* **27:**860–865

Yechiel, E., Edidin, M. 1987. Micrometer-scale domains in fibroblast plasma membranes. *J. Cell Biol.* **105:**755–760

Yguerabide, J., Stryer, L. 1971. Fluorescence spectroscopy of an oriented model membrane. *Proc. Natl. Acad. Sci. USA* **68:**1217–1221

Zlatonov, I.V., Foley, M., Birmingham, J., Garland, P.B. 1987. Developmental changes in the lateral diffusion of Leydig cell membranes measured by the FRAP method. *FEBS Lett.* **222:**47–50

Received 30 March 1992; revised 8 July 1992

Appendix

Fraction of dil that is Oriented

As indicated in Fig. 2, measurements of single-pixel intensity are taken at four tangential points on the image of a spheroplast: north (N), east (E), south (S) and west (W) with the N–S axis along the excitation polarization and the microscope emission polarizer oriented either parallel (‖) or perpendicular (⊥) to the N–S axis. The N and S measurements are averaged together and denoted as 'N'; the E and W measurements are averaged together and denoted as 'E'. The total observed fluorescence $F_{N,S}(\|, \perp)$ can be written as a linear combination of a contribution from dil that is highly ordered with respect to the spherical surface and a contribution that is randomly (isotropically) oriented:

$$k_{\|}F_N(\|) = P_N(\|) + \alpha_N R(\|)$$
$$k_{\|}F_E(\|) = P_E(\|) + \alpha_E R(\|)$$
$$k_{\perp}F_N(\perp) = P_N(\perp) + \alpha_N R(\perp)$$
$$k_{\perp}F_E(\perp) = P_E(\perp) + \alpha_E R(\perp)$$

$R(\|, \perp)$ and $P_{N,S}(\|, \perp)$ are the fluorescence intensities that would be observed from equal population sets of random and oriented dil, respectively. Factor $\alpha_{N,E}$ is the ratio of the number randomly oriented dil at the N or E positions to the number of highly ordered dil at the same positions. The concentration of the highly ordered dil is assumed to be the same at both N and E positions (since these dil are assumed to be uniformly dissolved in the membrane), but the concentration of randomly oriented dil is allowed to be position-dependent (since these dil may be aggregated in large clumps). We assume that the highly ordered dil molecules have their conjugated bridges all exactly parallel to the spherical surface. Factor $k_{\|,\perp}$ combine all the quantum efficiencies and polarization-dependent throughput factors relevant to the microscope detection system.

In these four equations, there are four unknowns: $k_{\|,\perp}$ (which we will eliminate) and $\alpha_{N,E}$ (which we solve for). $F_{N,S}(\|, \perp)$ is the input experimental data for each cell. $R(\|, \perp)$ and $P_{N,S}(\|, \perp)$ are "known" in principle and can be calculated from the theory presented in Axelrod (1979). However, they do depend on the selection of appropriate physical parameters describing a dil molecule. We choose these physical parameters here to be consistent with those chosen in Axelrod (1979) (based on steady-state polarization measurements of dil described there) and such that α_N and α_E, when averaged over all the cells, will be approximately equal. These parameters are: angle between the absorption dipole and the dil conjugated bridge $\theta = 20°$; angle between the emission dipole and the dil conjugated bridge $\theta' = 0°$; product of the rotational diffusion coefficient of dil in the membrane and its fluorescence lifetime $D_R\tau = 0.27$; a rotational diffusion coefficient of zero for randomly oriented dil; numerical aperture of the water-immersion objective = 1.20; and an effective half angle of observation from the equatorial plane of the cell $\gamma_o = 27°$ which arises from the finite square size of the CCD pixel (equivalent to 0.12 μm on a side) and the finite optical resolution (about 0.28 μm). The formalism in Axelrod (1979) takes into account all of these factors, all of which tend to depolarize the fluorescence, even if all the dil's were highly ordered.

Other depolarizing effects, such as nonspherical cell shape, submicroscopic membrane ripples, etc., are not taken into account. If they exist, they would make our estimate of the fraction of highly ordered dil an underestimate.